Preparation of transition metal–carbon material from polyacrylonitrile incorporated with inorganic salts

A. W. MORAWSKI*
Technical University of Szczecin, Institute of Inorganic Chemical Technology, ul. Pułaskiego 10, 70-322 Szczecin, Poland

M. UEDA, M. INAGAKI
Hokkaido University, Faculty of Engineering, Kita-ku, Sapporo 060, Japan

The incorporation of $CoCl_2$ and $FeCl_2$ into polyacrylonitrile (PAN) modified the carbonization behaviour and led to the development of carbon with a narrow pore radius ranging from 1.8–2.3 nm and a high surface area ranging from 182–190 $m^2 g^{-1}$. The carbon obtained was of better structural organization than from the original PAN, having an interlayer spacing, d_{002}, of 0.342 nm and a crystallite dimension along the c-axis, L_C, of 5.5–8.5 nm. The transition metals incorporated into carbon exhibited a strong resistance to hydrochloric acid solution treatment, suggesting high dispersion and strong anchoring of the transition metals in the carbon matrix. These non-crystallized and homogeneously distributed transition metals in carbon seem to promise some interesting applications, for example as supports in catalysis.

1. Introduction

Supported metal catalysts require a high degree of dispersion in order to maximize the catalytic activity per unit weight or volume. Carbon materials are usually used in heterogeneous catalysis as the supports for metals.

It is well known that activated carbons are produced from natural coal materials in an inert atmosphere, retaining their pore structure and properties [1]. The wide variety and reproducibility of their properties reflect the heterogeneous nature of most precursors of activated carbons [2, 3]. The catalysts prepared by impregnation of carbon supports with a solution of adequate inorganic salts, and by consequent reduction to metals, possess several disadvantages, the main one being the poor interaction of metal particles with the carbon support, which often results in the aggregation of the metal into bigger clusters. This leads, in most cases, to deactivation at a high temperature.

Recently, there has been interest in developing porous carbon as catalyst supports from polymers. The artificial carbon materials prepared from different synthetic precursors have many attractive properties. The polymer precursors are of special interest because of their well-defined macromolecular structure. The carbons prepared from these precursors can be expected to have reproducible characteristics and controlled pore size [4].

Several works have been performed on carbonization of polymer precursors, such as polyimides [5, 6] phenol resin [3, 7] and polyacrylonitrile [4, 8, 9]. Also several methods have been tried in order to modify the structure and properties of carbon materials to obtain better performance as supports. It was reported [10] that modification of the carbon structure can be reached by impregnation of the polymer precursor with a solution of some inorganic salts [11]. Solutions of different transition metal salts, such as $RuCl_3$, $MnCl_2$, $MoCl_2$, VCl_3, $FeSO_4$, $CuCl$, $ZnCl_2$, $FeCl_2$ and $CoCl_2$, were used as additives. The pyrolysis of polyacrylonitrile in the presence of ultrafine particles of metallic iron, nickel and copper has also been performed [9].

In the present work, a new method was proposed for *in situ* creation of transition metals (iron or cobalt) in carbon by reduction of inorganic salts with hydrogen which was generated during carbonization of polyacrylonitrile in an inert gas. The mixing of polyacrylonitrile with an inorganic salt in an organic solvent was employed to prepare the precursor, and the carbonization of the precursor was performed under controlled conditions, atmosphere, heating rate and residence time. Carbon materials with modified pore structure and also with strongly incorporated transition metal particles, were obtained. The transition metal/carbon support prepared will be a useful catalyst in industrial processes, for example ammonia synthesis, as has been proposed [9] and patented [12].

2. Experimental procedure

Polyacrylonitrile (PAN, 18 g) and $FeCl_2$ (1 g Fe) or $CoCl_2$ (1 g Co) were mixed by dissolving them into

---

* Author to whom all correspondence should be addressed.

dimethylformamide (DMF, 180 g). The solution was heated at a temperature of $\sim 70\,^\circ$C under stirring in a closed glass vessel for 3 h, to ensure complete dissolution of each component. Then, the solution was poured on to a flat glass vessel and DMF allowed to dry out for about 2 weeks in air. The platy block thus obtained was the PAN incorporated with an inorganic salt. For carbonization the precursors thus prepared were mechanically crushed to pieces of approximately 2×3 mm. The original PAN was also used as a control. About 1.2 g precursor was carbonized at $1000\,^\circ$C in a flow of high-purity argon with a flow rate of $5\,dm^3h^{-1}$. The heating rate was $200\,^\circ C\,h^{-1}$ and the sample was kept at $1000\,^\circ$C for 2 h. The cooling of the sample down to room temperature in the furnace took about 10h. The pH value of the decomposition gas was monitored.

The carbonized samples obtained were examined by X-ray diffraction (XRD, Rigaku Denki Co. Ltd, Japan) with CoK_α radiation, energy dispersive X-ray microanalysis (EDX, Jeol, JEO-2001SAJ, Japan) and scanning electron microscopy (SEM, Jeol, JSM-35CF, Japan). For SEM and EDX the specimens were mounted on a holder with a conductive carbon adhesive tape. The FeK_α (6.400 keV), CoK_α (6.930 keV) and ClK_α (2.622 keV) radiations were used for the distribution analysis of each element.

The average interlayer spacing, $d_{0\,0\,2}$, and crystallite dimension along the c-axis, $L_c(0\,0\,2)$, were determined from the $0\,0\,2$ diffraction line profile by referring to an inner standard of silicon.

The samples were also characterized by adsorption–desorption isotherms of nitrogen at a temperature of $-196\,^\circ$C. The specific surface area was calculated by the BET method at a relative gas pressure, p/p_0, up to 0.3 on the adsorption isotherm.

For estimation the HCl resistivity, the samples were treated with HCl solution (1:1) under magnetic stirring for 2 h at a temperature of about $50\,^\circ$C.

3. Results and discussion

The changes in pH value produced by the decomposed gases and changes in temperature of the sample during carbonization are shown in Fig. 1 as a function of heating time. Starting from around $200\,^\circ$C, the pH value detected in the effluent gases from all three samples increases abruptly to above 11. At high temperatures, the PAN sample gives basic gases during thermal decomposition and carbonization, which seems to be reasonable from its chemical composition. The pH value of the gases from the samples PAN–CoCl$_2$ and PAN–FeCl$_2$, decreases very rapidly above $500\,^\circ$C down to below 1 and increases again. During $1000\,^\circ$C holding, the gas becomes neutral, indicating the completion of out-gassing from these samples. The difference in the position of the two lines is caused by the difference in the melting points of CoCl$_2$ and FeCl$_2$.

The weight loss after the carbonization up to $1000\,^\circ$C from the sample PAN–FeCl$_2$ (61.12%) was lower than that of PAN–CoCl$_2$ (62.48%) and PAN (66.8%). These observations suggest different carbon-
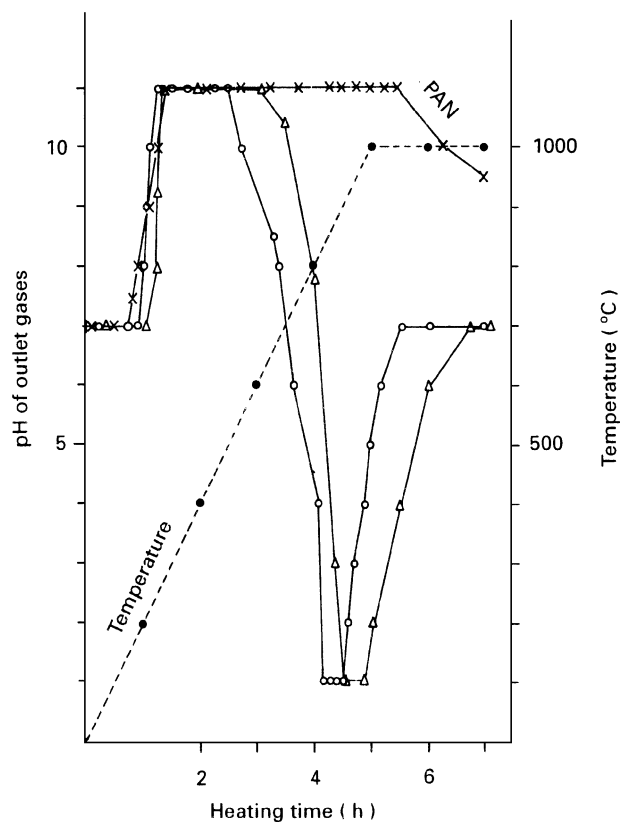

Figure 1 Changes in pH value produced by out-gassing during carbonization of the samples. ($\times$) PAN, ($\triangle$) PAN–CoCl$_2$, ($\bigcirc$) PAN–FeCl$_2$, ($\bullet$) temperature.

TABLE I X-ray parameters, specific surface area and dominant radius of pores

Precursor name	$d_{0\,0\,2}$ (nm)	$L_c(0\,0\,2)$ (nm)	Surface area by $N_2(m^2g^{-1})$	Dominant pore radius (nm)
PAN	0.358	1.4	154	< 1.0
PAN–CoCl$_2$	0.342	5.5	190	2.3
PAN–FeCl$_2$	0.342	8.5	182	1.8

ization processes in these three precursors, which surely affects the structure and texture of the resultant carbons.

The X-ray parameters, $d_{0\,0\,2}$ and $L_c(0\,0\,2)$, calculated from the $0\,0\,2$ diffraction profile are summarized in Table I. The X-ray data on the carbonized PAN, very broad and weak $0\,0\,2$ diffraction profile, large $d_{0\,0\,2}$ and small crystallite size, $L_c(0\,0\,2)$, indicate that the sample gave poorly organized carbon, in accordance with the results published in the literature. The incorporation of inorganic salts, CoCl$_2$ and FeCl$_2$, into PAN produces carbons with much lower $d_{0\,0\,2}$ and relatively larger $L_c(0\,0\,2)$ than PAN itself, suggesting much better organization. It is worthwhile to point out that the X-ray parameters for both carbons PAN–CoCl$_2$ and PAN–FeCl$_2$ are practically the same as the PAN-based carbon fibres heat treated up to $2500\,^\circ$C ($L_c(0\,0\,2) = 7.0$–8.0 nm, $d_{0\,0\,2} = 0.342$ nm) even though they have been heat treated only up to $1000\,^\circ$C [13].

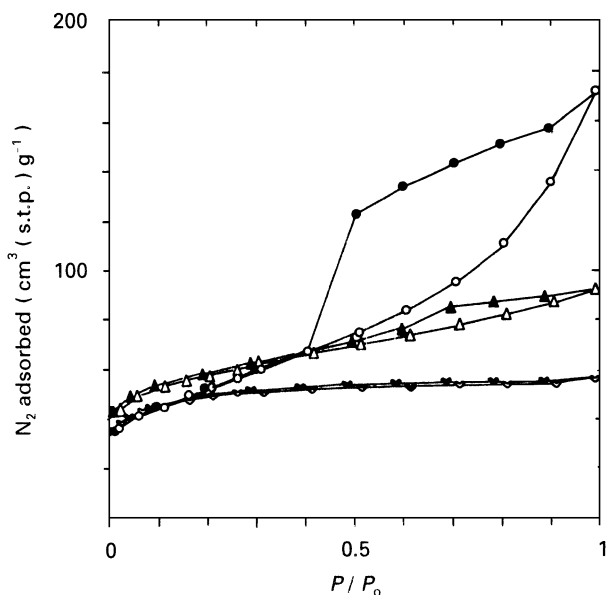The adsorption–desorption isotherms of nitrogen at $-196\,^\circ$C on three carbons are shown in Fig. 2. The

Figure 2 Adsorption–desorption isotherms of nitrogen gas at −196 °C on the samples carbonized up to 1000 °C. (♡, ♥) PAN, (△, ▲) PAN–CoCl$_2$ and (○, ●) PAN–FeCl$_2$. (♡, △, ○) *adsorption*, (♥, ▲, ●) *desorption*.
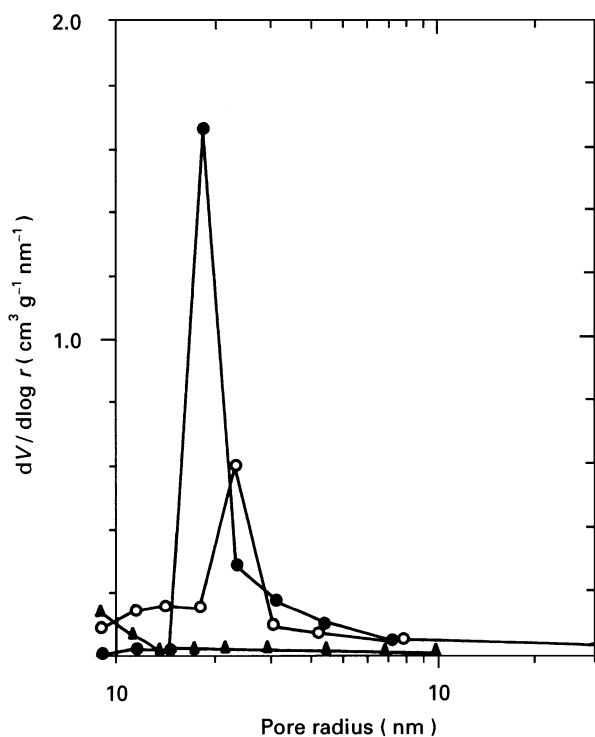
Figure 3 Pore volume distribution determined from the adsorption of nitrogen at −196 °C. (▲) PAN, as-carbonized; (●) PAN–FeCl$_2$, as-carbonized; (○) PAN–FeCl$_2$, after HCl treatment.

isotherm of the control carbon obtained from PAN belongs to Type I; the amount of adsorbed nitrogen sharply increases at low relative pressures and reaches practically a plateau. This Type I isotherm has often been observed when the adsorbent is microporous and also when the width of pores is up to two molecular diameters of the adsorbate. The shape of the adsorption isotherms of the carbons PAN–CoCl$_2$ and PAN–FeCl$_2$ is quite different in character from that of the PAN. These isotherms may be classified into pseudo-Type II; very rapid adsorption of nitrogen gas

at low relative pressures and a remarkable hysteresis loop at high relative pressures (Type H3). A capillary condensation of nitrogen in the pores is reasonably supposed for these two samples. The amount of condensed nitrogen is larger in the carbon PAN–FeCl$_2$ than in PAN–CoCl$_2$. The desorption took a much longer time than the adsorption, especially at the transition in p/p_0 from 0.5 to 0.4 corresponding to a sharp desorption edge of the hysteresis loop. Fig. 3 shows examples of pore distribution curves versus pore radius for the PAN–FeCl$_2$ series and control PAN determined by Barrett *et al.*'s (BHJ) method [14] from the observed isotherms. The development of a new region of micropores can be seen on the carbons prepared under the incorporation of inorganic salts, to be much clearer in the carbon PAN–FeCl$_2$ than in PAN-CoCl$_2$. The distribution of pores in the samples after treatment with HCl did not show any change in pore distribution. Surface areas also remain intact after HCl treatment of the two carbon samples, PAN–CoCl$_2$ and PAN–FeCl$_2$. The development of a new region can be concluded to be due to the incorporation of CoCl$_2$ and FeCl$_2$. The dominant radius of newly developed pores is about 1.8 and 2.3 nm (Table I), respectively, which is on the border between micro- and mesopores. On the control sample PAN, there are no pores in this size region, only those with a size less than 1.0 nm.

Fig. 4a and b show diffractograms of the samples PAN–CoCl$_2$ as-carbonized and treated by HCl solution, respectively. In the as-carbonized sample presented are phases of metallic cobalt, CoO, Co$_2$O$_3$, Co$_3$O$_4$ and carbides. Three possibilities for the formation of cobalt oxides in this carbon must be taken into account, oxidation during carbonization of the sample by oxygen presented in the PAN molecules, also by oxygen in the residue of DMF used as solvent, and oxidation in air after carbonization. The treatment of this sample by HCl solution removes almost all the metallic cobalt, cobalt oxides and carbides. There might be only a minute amount of carbides left. Fig. 4c and d present the diffractograms of the samples derived from PAN–FeCl$_2$. In the as-carbonized sample, metallic iron, Fe$_2$O$_3$, Fe$_3$O$_4$ and carbides are detected. After HCl treatment, all these impurity phases were practically removed.

The scanning electron micrographs and EDX data on the samples as-carbonized and after HCl treatment are summarized in Figs 5–8. The morphology of carbonized PAN incorporated with CoCl$_2$ or FeCl$_2$ is quite different in character from the PAN itself. The PAN as-carbonized (Fig. 5) has apertures of no regular shape, which vary from an oblong to a round, with smooth walls. In the carbon prepared from PAN–FeCl$_2$ (Fig. 6), there are no large cavities nor apertures. They are rather in the shape of blocks with sharp edges. This characteristic shape was not disturbed by the carbonization process, which could be called a "shape memory". The blocks are covered by minute particles, which practically disappeared after HCl treatment (Fig. 6c and d). The shape of blocks is also modified by HCl treatment (Fig. 6c and 6d), the edges of carbon grains appear to have been attacked. The
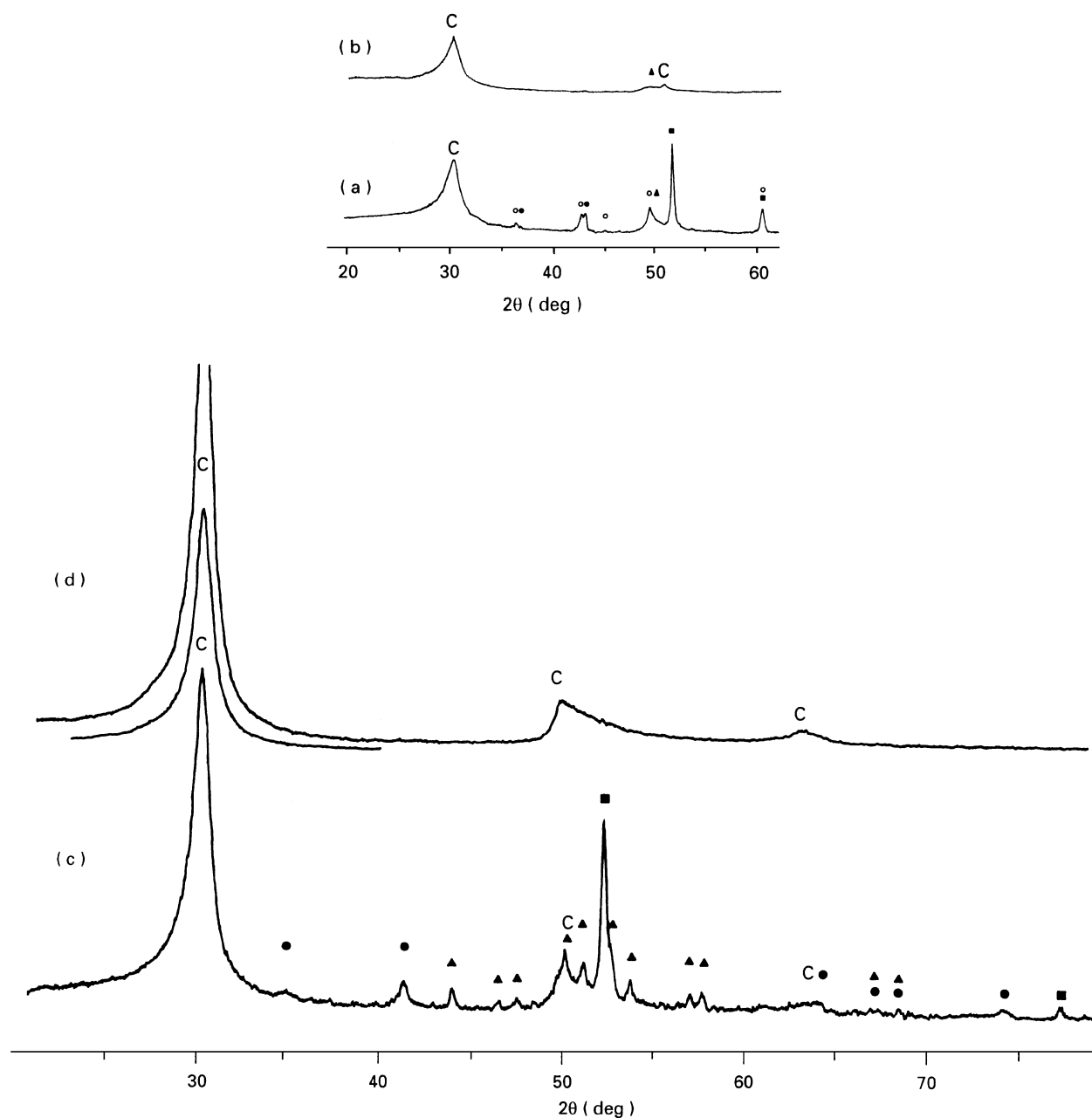
Figure 4 X-ray diffraction patterns of the samples. CoK_α radiation. (a) PAN–CoCl$_2$, as-carbonized; (b) PAN–CoCl$_2$, after HCl treatment. (○) CoO, Co$_2$O$_3$; (●) Co$_3$O$_4$; (▲) carbides; (■) Co; C, carbon. (c) PAN–FeCl$_2$, as-carbonized; (d) PAN–FeCl$_2$, after HCl treatment. (○) Fe$_2$O$_3$; (●) Fe$_3$O$_4$; (▲) Fe–C, Fe$_2$C, Fe$_3$C, Fe$_2$C$_5$; (■) Fe; C, carbon.
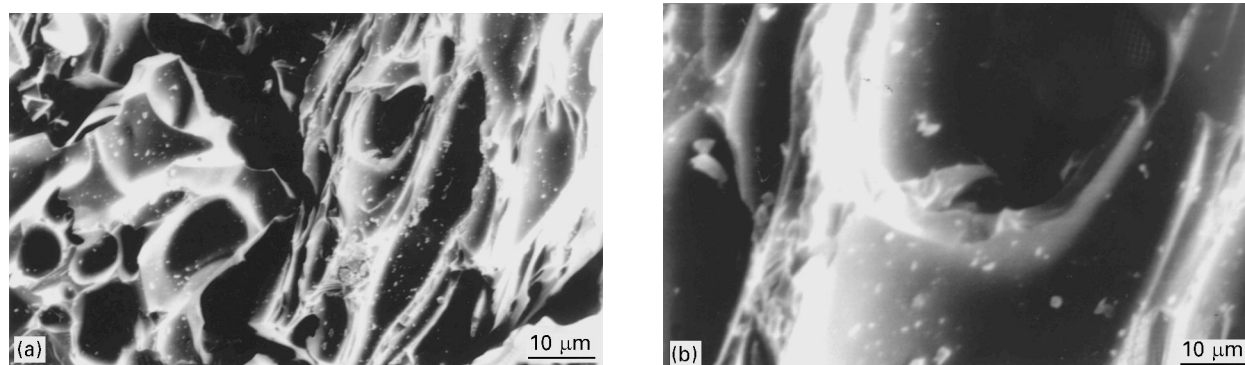

Figure 5 Scanning electron micrographs of PAN as-carbonized.

same observations on the PAN–CoCl$_2$ sample were also obtained by SEM.

The EDX measurements of cobalt and iron line profiles on the above samples are in good agree-

ment with SEM observations. In the flat grains of sample "PAN–CoCl$_2$" (Fig. 7a), a practically constant distribution of cobalt, with a slightly higher concentration on the edges, is noticed (Fig. 7b). The
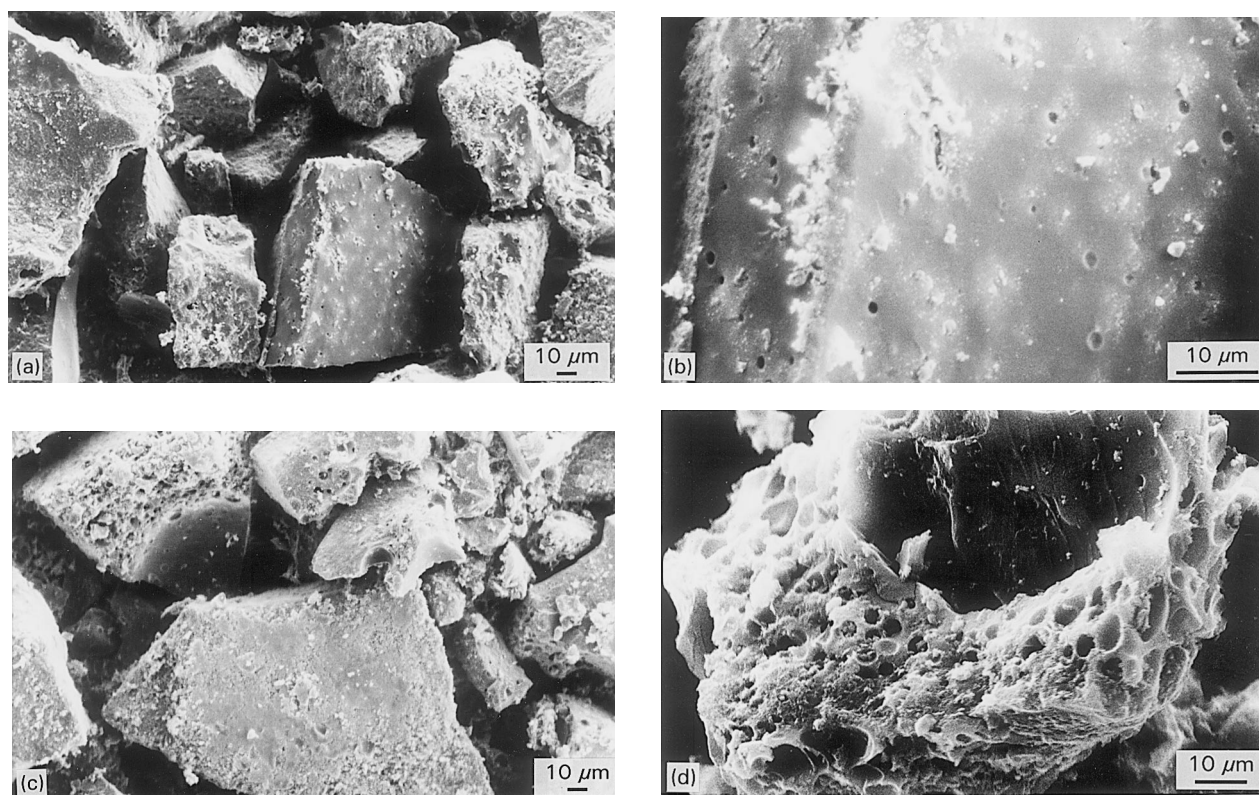
Figure 6 Scanning electron micrographs of the series sample PAN–FeCl$_2$: (a,b) as-carbonized, (c, d) after HCl treatment.
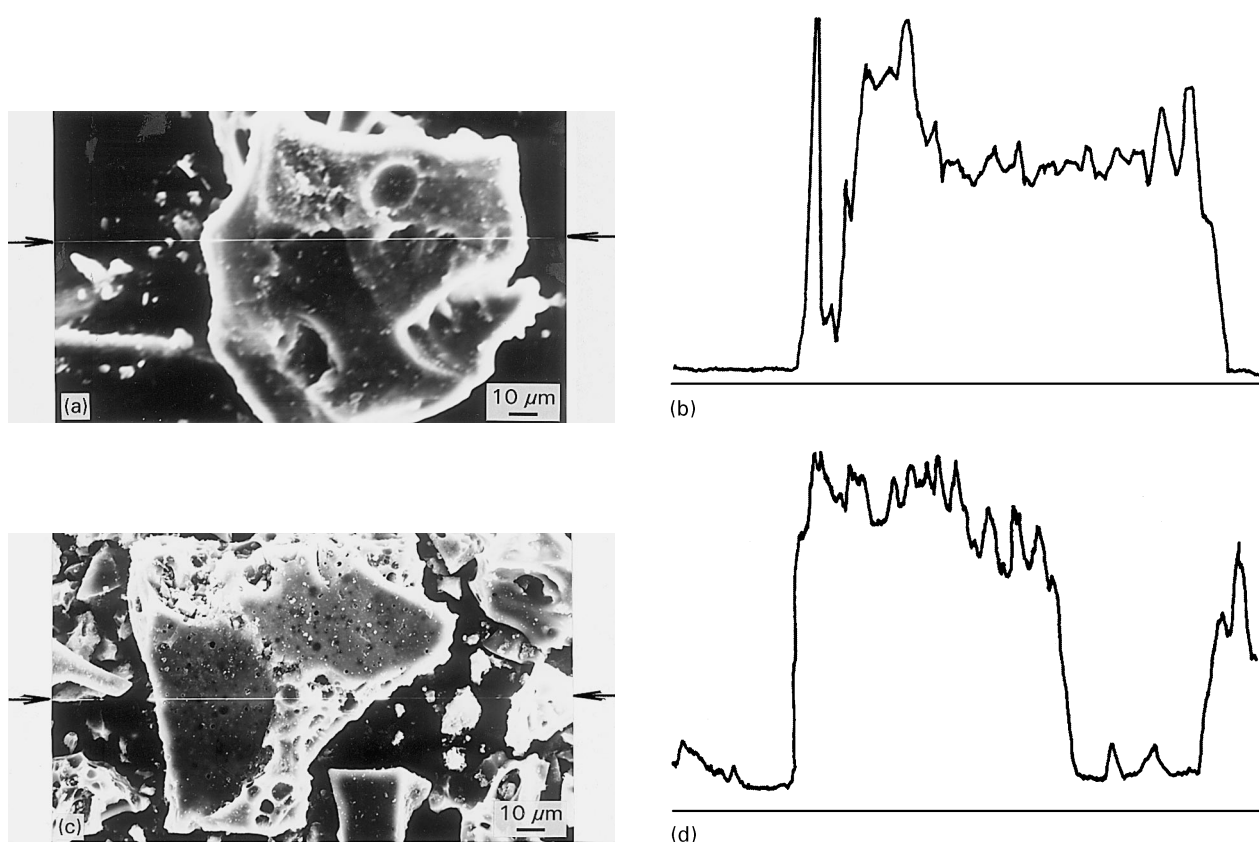

Figure 7 Distribution of cobalt along the line indicated by arrows on the grains of the PAN–CoCl$_2$ sample: (a) as-carbonized, scanning electron micrograph; (b) as-carbonized, distribution of CoK_α line; (c) after HCl treatment, scanning electron micrograph; (d) after HCl treatment, distribution of CoK_α line.

intensity of the chlorine line along the particle (Fig. 7c) indicates a very low concentration of chlorine (line of weak intensity above the background) in the sample. The HCl (1:1) treatment did not change the equal distribution of cobalt; only the total amount of cobalt decreases slightly (Fig. 7d), compared with the intensity of the cobalt line detected before acid treatment (Fig. 7b).
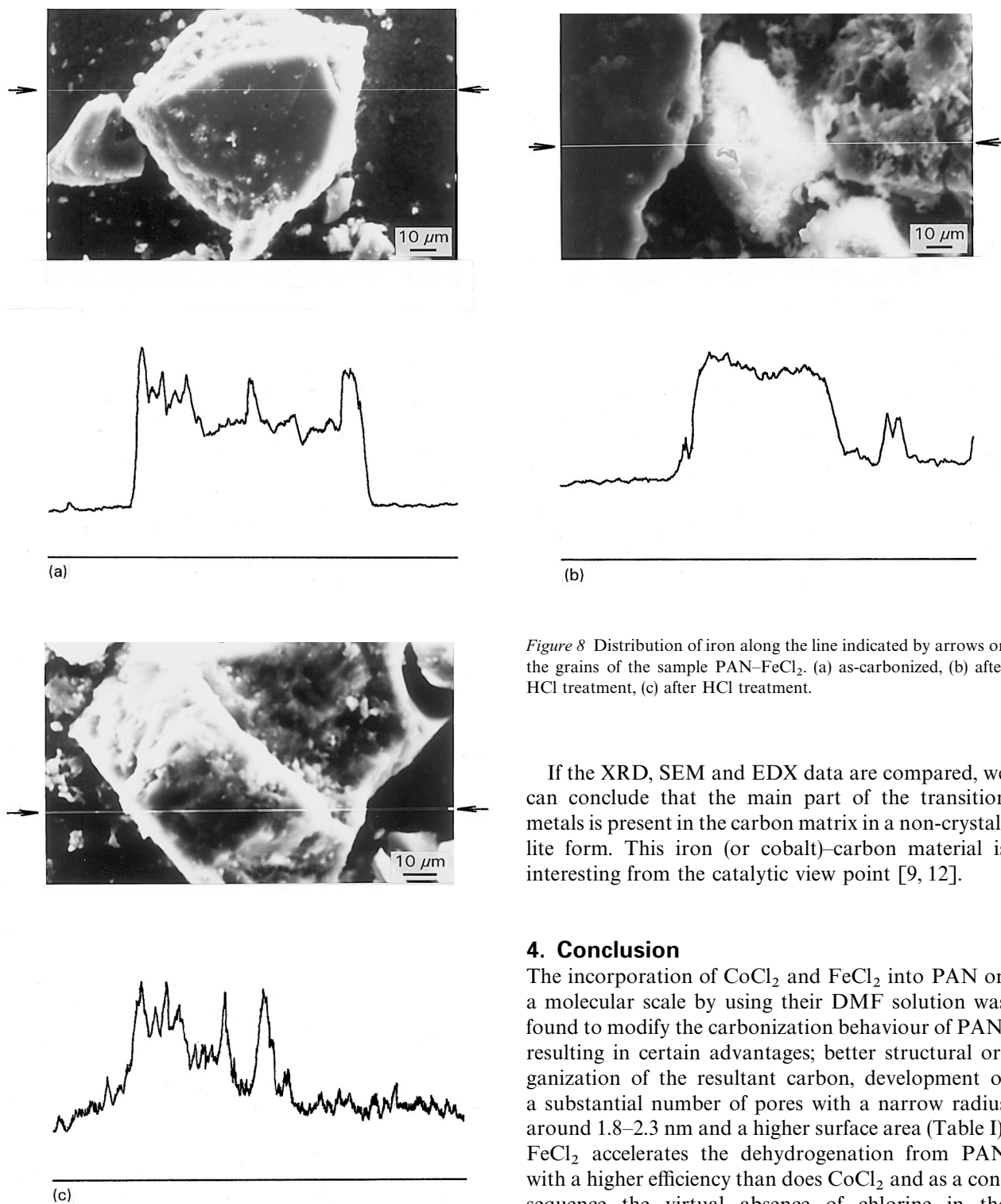
Figure 8 Distribution of iron along the line indicated by arrows on the grains of the sample PAN–FeCl$_2$. (a) as-carbonized, (b) after HCl treatment, (c) after HCl treatment.

If the XRD, SEM and EDX data are compared, we can conclude that the main part of the transition metals is present in the carbon matrix in a non-crystallite form. This iron (or cobalt)–carbon material is interesting from the catalytic view point [9, 12].

4. Conclusion

The incorporation of CoCl$_2$ and FeCl$_2$ into PAN on a molecular scale by using their DMF solution was found to modify the carbonization behaviour of PAN, resulting in certain advantages; better structural organization of the resultant carbon, development of a substantial number of pores with a narrow radius around 1.8–2.3 nm and a higher surface area (Table I). FeCl$_2$ accelerates the dehydrogenation from PAN with a higher efficiency than does CoCl$_2$ and as a consequence the virtual absence of chlorine in the transition metal/carbon support was confirmed by EDX. Low-temperature dehydrogenation of PAN by FeCl$_2$ and CoCl$_2$ may assist the growth and alignment of condensed aromatic rings and may be advantageous in the development of micropores. The transition metals incorporated in the carbon material may allow distinct potential uses, for example in catalysis, because of the high dispersion and high concentration of anchored metal particles.

The distributions of iron along the grains of the PAN–FeCl$_2$ sample (Fig. 8a) show a high concentration, even in the centre of the grains. The iron located at the edge of the grain is easily attacked by HCl solution, as shown in Fig. 8b and c, no iron was found on the edges. It must be pointed out, however, that even after HCl treatment the grains still possess a very high concentration of iron. Some diversity of iron concentration is found; the grain in Fig. 8c has a very low concentration and also an inhomogeneous distribution of iron in comparison with that in Fig. 8b. The distribution of chlorine in the PAN–FeCl$_2$ sample confirmed the complete reduction of FeCl$_2$ during carbonization.

References

1. OM P. MAHAJAN, *Carbon* **29** (1991) 737.
2. D. S. CAMERON, S. J. COOPER, I. L. DODGSON, B. HARRISON and J.W. JENKINS, *Catal. Today* **7** (1990) 113.
3. B. McENANEY, I. M. PICKUP and L. BODSWORTH, *ibid.* **7** (1990) 299.
4. A. W. MORAWSKI, K. KAŁUCKI, M. NAKASHIMA and M. INAGAKI, *Carbon*, **32** (1994) 1457.
5. M. INAGAKI, L.-J. MENG, T. IBUKI, M. SAKAI and Y. HISHIYAMA, *ibid.* **29** (1991) 1239.
6. H. HATORI, Y. YAMADA, M. SHIRAISHI and Y. TAKAHASHI, *ibid.* **29** (1991) 679.
7. M. INAGAKI and M. NAKASHIMA, *ibid.* **30** (1992) 1135.
8. N. SONOBE, T. KYOTAMI and A. TOMITA, *ibid.* **26** (1988) 573.
9. T. WATANABE, Y. OHTSUKA and Y. NISHIYAMA, *ibid.* **32** (1994) 329.
10. J. J. FREEMAN, F. G. R. GIMBLETT and K. S. W. SING, *ibid.* **27** (1989) 85.
11. J. C. CAVALIER, E. CHORNET, B. BEAUREGARD and G. COQUARD, *ibid.* **16** (1978) 21.
12. K. KAŁUCKI, A. W. MORAWSKI and W. ARABCZYK, *Polish Patent* P.300687 (1993).
13. W. KOWBEL, E. HIPPO and N. MURDIE, *Carbon* **27** (1989) 219.
14. E. P. BARRETT, L. G. JOYNER and P. P. HALENDA, *J. Amer. Chem. Soc.* **73** (1951) 373.